Friction **10**(9): 1285–1304 (2022) ISSN 2223-7690
https://doi.org/10.1007/s40544-021-0589-y CN 10-1237/TH
Review Article

Tailored surface textures to increase friction—A review

Henara L. COSTA[1,*], **Jörg SCHILLE**[2], **Andreas ROSENKRANZ**[3,*]

[1] *School of Engineering, Surface Engineering Group, Universidade Federal do Rio Grande, Rio Grande 96203900, Brazil*

[2] *University of Applied Sciences Mittweida, Laserinstitut Hochschule Mittweida 09648, Germany*

[3] *Department of Chemical Engineering, Biotechnology and Materials, University of Chile, Santiago 8370459, Chile*

Received: 14 October 2021 / Revised: 10 November 2021 / Accepted: 12 December 2021

Abstract: Surface textures with micro-scale feature dimensions still hold great potential to enhance the frictional performance of tribological systems. Apart from the ability of surface texturing to reduce friction, surface textures can also be used to intentionally increase friction in various applications that rely on friction for their adequate functioning. Therefore, this review aims at presenting the state-of-the-art regarding textured surfaces for high-friction purposes. After a brief general introduction, the recent trends and future paths in laser surface texturing are summarized. Then, the potential of surface textures to increase friction in different applications including adhesion, movement transmission and control, biomimetic applications, and road-tire contacts is critically discussed. Special emphasis in this section is laid on the involved mechanisms responsible for friction increase. Finally, current short-comings and future research directions are pointed out thus emphasizing the great potential of (laser-based) surface texturing methods for innovations in modern surface engineering.

Keywords: surface texturing; tribology; laser processing; friction increase

1 Introduction

Important aspects of our daily life are governed by tribological phenomena and processes involving friction, wear, and lubrication. Tribology is a rather broad and multi-disciplinary topic, spreading from traditional engineering applications to modern aspects of biotribology. More traditional areas of tribological research often relate to mechanical components (gears, bearings, brakes, piston rings, tires, among others) and their energy efficiency [1–5]. Modern tribological research fields are connected to nanotechnology [6–9] and/or biotribology [10–13], which deals, for instance, with the application of lipstick [14, 15], the usage of contact lenses [16, 17], skin comfort during shaving [18], tactile perception [19, 20], the proper functioning of artificial knee and hip implants [21–24], or oral tribology, which assesses the perceptions of sensations/feelings induced through the interaction of food and beverages with the mouth's components and saliva [25–27].

Scientists around the globe explore new ways to reduce friction and wear as a key strategy to increase the resulting energy efficiency. While friction directly correlates with the resulting mechanical and energy losses and, therefore, energy consumption, the reduction of wear is essential to ensure long-lasting components, which do not lose their function during use [3, 4]. To reduce friction and wear, the tribological interface, which consists of two counter-bodies rubbing against each other under a certain load and velocity, needs to be considered. Different approaches can be pursued to optimize and tailor the tribological response of a system. In this regard, lubrication strategies based upon new lubricants such as water [28–30] or ionic liquids [31, 32], tailored additives [33–35] or even solid lubrication [36–39] are subject of ongoing research activities. Moreover, the deposition of low

* Corresponding authors: Henara L. COSTA, E-mail: henaracosta@furg.br; Andreas ROSENKRANZ, E-mail: arosenkranz@ing.uchile.cl

shear-strength coatings, particularly by physical or chemical vapor deposition [40], has been proven to be an efficient way to control friction and wear. Due to the direct contact of both rubbing surfaces through their surface micro-asperities, the generation of surface textures/patterns thus modifying the involved surface topography is another powerful approach to reduce friction and wear.

The first studies in this context date back to Hamilton [41] and Anno [42], who demonstrated beneficial effects when using surface textures in mechanical seals. The overall topic experienced a renaissance in the 90s by the works of Etsion and his co-workers, who ultimately verified that laser surface texturing (LST) is an excellent method to improve the tribological performance of different mechanical components [43–45]. This led to tremendous subsequent attention in the tribological community, with numerous contributions across all lubrication regimes ranging from dry friction [46, 47] over boundary [48, 49] and mixed lubrication [50–52] to elastohydrodynamic [53–55] and full-film hydrodynamic lubrication [56, 57], as well as under starved conditions of lubricant supply [58, 59]. Today, the effects of surface textures on the tribological performance under different lubrication regimes and working conditions are reasonably well explored and understood. For dry conditions, surface textures help to reduce the real area of contact and stiction as well as offer the possibility to store wear debris [46, 47, 60–63]. Under boundary lubrication, surface textures additionally act as a secondary oil source [64] and may help to generate beneficial boundary layers (pressure-induced tribo-layer formation) [65–67]. In the case of mixed lubrication, surface textures store oil and wear debris as well as help to build up an additional hydrodynamic pressure [50–52]. Concerning elastohydrodynamic and hydrodynamic lubrication, surface textures build up pronounced additional pressures, which help to separate both rubbing surfaces [56, 57]. In addition, textures may beneficially influence cavitation thus improving the frictional characteristics [68, 69]. A number of review papers, which describe how surface textures reduce friction and wear and summarize the underlying mechanisms, have been published [43, 70–74]. Although having different scopes, all these reviews have in common that they mainly assess the textures' ability to reduce friction and wear.

Despite the general paradigm that friction is an aspect to be reduced, a careful consideration of the working principle of different machine components makes evident that friction is essential for different machine components and frequently needed to induce and/or maintain certain functionalities. In a world without friction, humans would not be able to walk or, once in motion, they would not be able to slow down and stop their movement. A closer look into brakes [75, 76] and clutches [77, 78] reveals that they rely on friction; a certain value of the acting coefficient of friction (COF) must be achieved to ensure their proper function. When aiming at improving their performance, the COF rather needs to be increased, which demonstrates that it can be partially beneficial to intentionally increase friction. To achieve this goal, the control of the involved surface topography may be considered as a key route. For example, for elastic surfaces, rationally designed surface textures may increase the real area of contact and, therefore, the adhesion component of friction [79]. This would increase the overall COF. In plastic contacts, a rougher topography may increase the deformation component of friction [80]. Moreover, by designing and aligning the surface topography of both surfaces, mechanical interlocking can be achieved thus increasing static as well as kinetic friction [46].

Without any doubt, significantly more research work has been addressing the effect of surface textures with the overall intention to reduce friction and wear. This may relate to the functions of the produced surface textures including the reduction of the real area of contact, the storage of wear debris and oil as well as the additional pressure build-up, which all aim at reducing friction and/or wear. Limited research has dealt with the possibility of intentionally increasing friction by surface texturing while maintaining wear at a low level. Especially, the combination of surfaces enabling high friction and low wear (durability) is tricky but bears tremendous potential in different high-friction machine components. Therefore, this review article aims to summarize the existing state-of-the art on surface texturing for high-friction purposes with a particular emphasis on the involved mechanisms. Afterwards, we derive the current shortcomings and future research trends before presenting some concluding remarks.

2 Recent trends in laser surface texturing

Although many techniques have been used to texture surfaces [81], laser surface texturing (LST) undoubtedly presents the most widespread use in real practice with many successful applications. The dimensions of the textures range from nanometer (nm) to micrometer (μm) thus providing the ability to tailor and control the characteristic micro-topography but also physico-chemical properties of solid surfaces. So far, LST has been used for functional enhancement concerning, i.e., self-cleaning [82], anti-icing [83], or anti-bacterial [84] surfaces. Actually, there is an ongoing trend for mimicking natural concepts by LST with great potential to be used for biomimetic surface functionalities, interfaces and products [85]. It has been experimentally validated that ripples can function as grating structure diffracting light for optical effects (Fig. 1(a)) [86]. Multi-scale laser textures can induce water-repellent and self-cleaning behavior (Fig. 1(b)) [86], while rib-shaped groove structures (Riblet, Fig. 1(c)) [86] are beneficial to reduce wall shear stress and skin friction drag on solid surfaces in turbulent flows. A recent study reports on improving boiling heat transfer for laser-textured surfaces (Fig. 1(d)) [87].

The described examples have in common the use of ultrashort pulsed (USP) laser systems. In addition to efficient material removal, their main advantage is the reduced thermal load to the substrates allowing for the fabrication of (almost) melt-free microscale surface structures. In this regard, surface textures such as grooves and micro holes/dimples can be produced by direct laser ablation. Moreover, rather (sub-) micrometer features (laser induced periodical surface structures (LIPSS) [88–90] or cone-like protrusions (CLP) [86, 91–93]) can be created from self-reorganizing and surface feedback driven processes. Two different types of LIPSS have been reported [90, 93]: (1) classical ripples or rather low-spatial-frequency LIPSS (LSFL) with a spatial period close to the wavelength ($\Lambda_{\mathrm{LSFL}} \lesssim \lambda$) and, in most cases, perpendicularly oriented to the

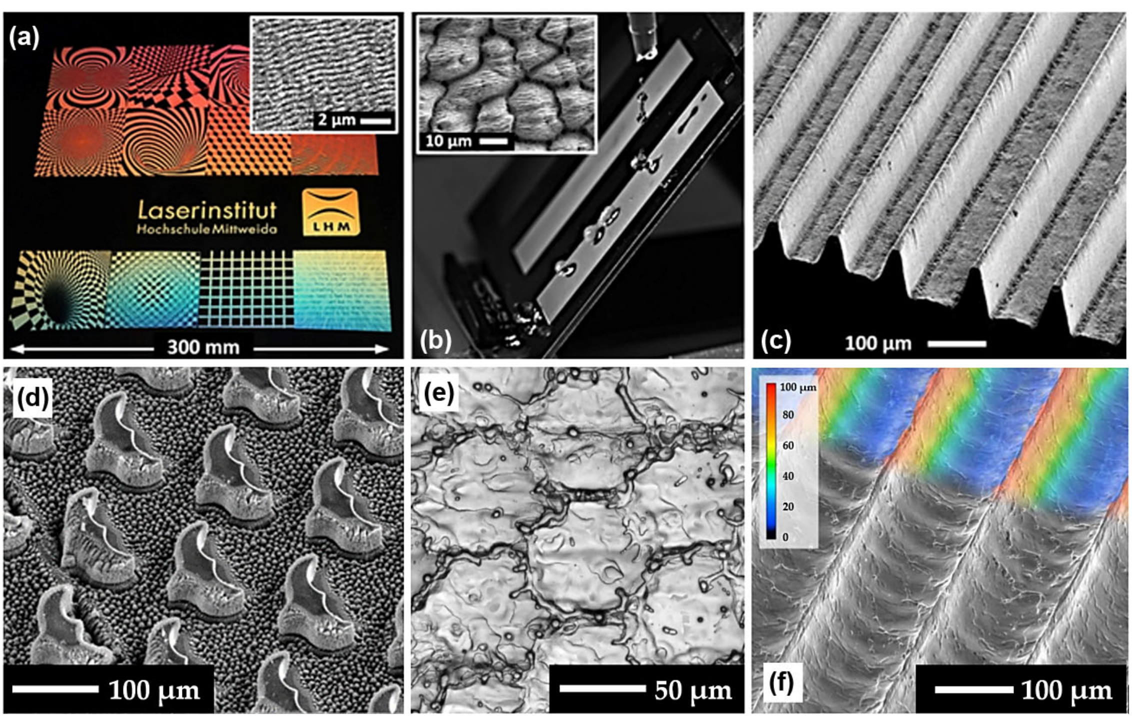

Fig. 1 LST for surface functionalization: (a) optical effects by ripple texture for diffracting light [86], (b) multi-scale surface texture for water-repellent hydrophobic surface conditions [86], (c) shark-skin inspired Riblet texture to reduce skin friction drag on surfaces in turbulent flows [86], (d) laser textures for improving boiling heat transfer [87], (e) dimples for static friction increase [100], (f) U-shaped Riblet produced by high-speed scanning a 3 kW CW laser beam. Reproduced with permission from Ref. [86], © The Authors 2020; Ref. [87], © ASME 2018; Ref. [100], © The Authors 2014.

polarization of the laser radiation, and (2) high-spatial-frequency LIPSS (HSFL) with a spatial period considerably smaller than the wavelength ($\Lambda_{HSFL} < \lambda/2$) and parallel oriented to the polarization of the incoming laser beam. The characteristic feature topography can be controlled by the laser processing conditions, i.e., wavelength, fluence, spatial pulse overlap, number of scan crossings, angle of incidence, among others [94–99].

In many studies, the applied average laser power was relatively low (about a few Watts), which limited the achievable processing speed and throughput. Typically, the processing speed was in the range of $mm \cdot s^{-1}$ and thus the laser texturing of areas in the range of cm^2 for functional testing required hours to days, which is a clear drawback to bring the promising LST technology to industrial production. However, the amazing progress of the USP laser technology reaching kilo Watt class level [101, 102] in combination with innovative processing strategies will allow unprecedented production rates in the range of $m^2 \cdot min^{-1}$ in near future [86, 92, 103, 104].

Nanosecond pulsed (ns-pulsed) and continuous wave (CW) lasers are an alternative to USP lasers, which can supply higher laser powers at cheaper investment costs. However, when compared with USP laser, their great drawback is the need for higher optical energy for material ablation thus causing a much stronger heat impact to the substrates, accompanied by material melting and enlarged heat affected zones. This considerably reduces the microstructural resolution and quality of the surface textures, thus hindering an extensive implementation of ns-pulsed and CW lasers in micro-machining and LST. However, a number of papers report on dimples fabricated by pulsed lasers surrounded by molten walls, (Fig. 1(e)) [100], which have been found beneficial for increasing static friction of tribological systems [100]. For micro-scale grooves, the highest processing speed was achieved so far by using a single-mode CW fiber laser in combination with polygon scanner-based laser beam deflection. Therewith, even in case of extremely high 3 kW CW laser powers applied in micro-processing, the thermal load to the material was reduced by distributing the irradiated optical power over large areas by ultrafast, in fact several hundreds of meters per second, laser beam moving. A potential application for high-power CW lasers in LST has been validated by the fabrication of U-shaped Riblet structures (Fig. 1(f)).

3 Tailored surface textures to increase friction

3.1 Laser surface texturing of fairly hard tribological contacts

Tribological tests of textured surfaces almost always intend to evaluate their ability to reduce friction. Only a few studies report that friction increase due to surface texturing could be desirable. Xing et al. [105] laser-textured an Al_2O_3/TiC ceramic composite aiming to increase friction and reduce wear. They generated straight and zig-zag groove-like textures on Al_2O_3/TiC ceramics with variable periodicities while keeping the widths and depths constant (40–50 μm). Irrespective of the sliding speed and the grooves' periodicity as well as geometry, textures increased the resulting COF and simultaneously maintained wear at an acceptably low level. With respect to the groove geometry, zig-zag textures with smaller periodicities induced the greatest increase of the resulting COF. The increase in friction was attributed to the roughening of the ceramic specimens with surface texturing, leading to micro-cutting of the groove edges, while the entrapment of wear debris within the grooves was responsible for reducing wear [105]. Similar effects of increased friction due to increased roughness induced by texturing have also been observed for other materials. Surface texturing by maskless electrochemical texturing has resulted in roughening of steel specimens, leading to higher friction under boundary lubrication conditions. In addition, the entrapment of wear debris within the textures was verified, reducing the wear rates by around 39% [48].

Numerous studies have addressed the possibility to increase friction using LIPSS fabricated by ultra-short pulse laser processing on various substrate materials. Eichstädt et al. [106] studied laser processing parameters such as number of pulses, repetition rate, and pulse energy to fabricate homogeneous, large-scale LIPSS on a flat single-crystalline silicon mirror substrate. Ball-on-disk experiments with low normal loads up to 25 mN (ball's sliding direction perpendicular to the LIPSS) verified a maximum friction increase by a factor of 1.6. This was traced back to the changed surface topography and potential changes in the underlying surface chemistry/crystalline state. Rung et al. [107] produced low frequency LIPSS and micro-channels fabricated by ultra-short pulse laser processing on 100Cr6 steel (Figs. 2(a)–2(d)). Tribological experiments were parallel and perpendicular with respect to the grooves' direction (Figs. 2(e) and 2(f)). Under dry sliding, LIPSS induced higher friction irrespective of orientation and counter material used. Since no detailed explanation has been given by the authors, we can just hypothesize that the increased surface roughness of the low-frequency LIPSS was responsible for this frictional increase. However, this assumption needs to be backed up with further tribological testing and materials characterization. Nevertheless, ultra-short laser processing is an interesting approach to tune/increase friction due to the achievable aspect ratio between the depth and width of the textures of about 1:1.

Van der Poel et al. [108] fabricated single-scale and multi-scale grooves on CoCrMo alloys. By changing the polarization of the laser beam, they generated triangular nano-pillars. Compared to the polished reference, all textured surface increased friction. The most pronounced effects were found for the single- and multi-scale grooves. The authors explained the observed frictional behavior by the modified surface topography. Alves-Lopes et al. [109] fabricated LIPPS in silicon by direct femtosecond laser writing. The reference showed a stable COF of about 0.12–0.14 without pronounced running-in and wear features, which was traced back to the absence of plastic deformation, adhesive marks, and ploughing (mild oxidative wear). In contrast, LIPSS demonstrated a 3.5-fold increase in friction with slightly higher values for the perpendicular direction. This experimental trend was explained by the considerably rougher LIPSS and their structural degradation during running-in, which went hand in hand with plastic deformation and ploughing marks. Moreover, a higher degree of oxidation was verified for the LIPSS by comparing the content of oxygen present for the laser textured and untreated surfaces, which explains, together with the other observed wear features, the increased COF values [109]. These studies evidence that for applications aiming to increase friction while maintaining low wear LIPSS stands out as a particularly suited texturing technique. Table 1 summarizes the texture geometries, sliding conditions and levels of friction increase achieved in basic laboratory tests of LIPSS as friction-increasing strategy.

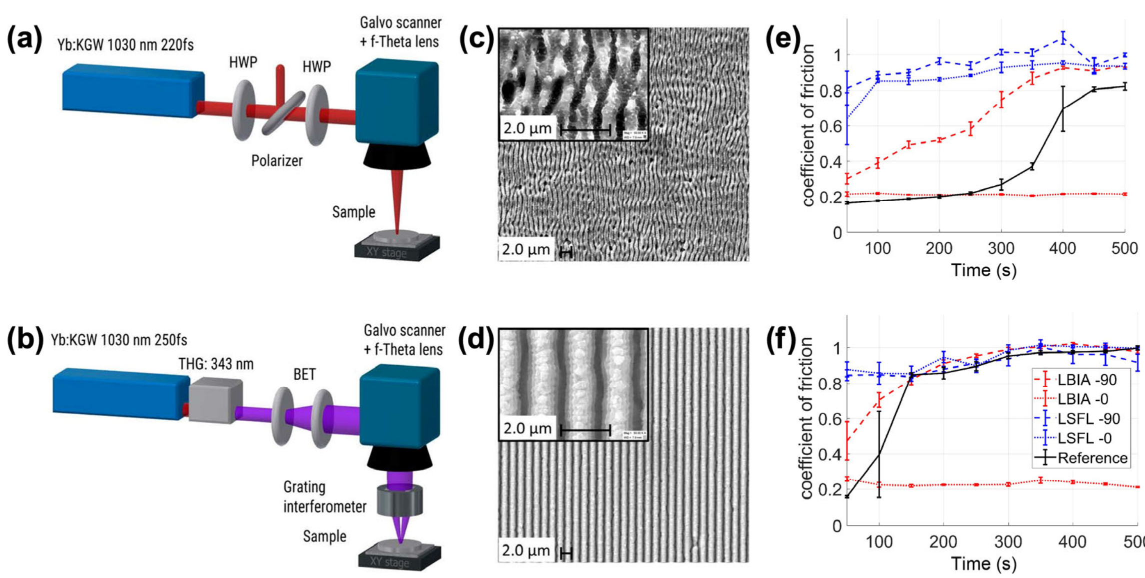

Fig. 2 (a, b) Ultra-short pulse laser texturing strategies to fabricate (c) low frequency LIPSS and (d) micro-channels on 100Cr6 steel. (e, f) Temporal evolution of the COF for low frequency LIPSS and micro-channels depending on the sliding direction for an applied normal load of (e) 50 and (f) 200 mN, respectively. In this regard, 0 reflects a sliding direction parallel to the LIPSS and groves, while 90 indicate the perpendicular sliding direction. The abbreviation "LSFL" stands for the low frequency LIPSS, whereas "LBIA" refers to the micro-channels. Reproduced with permission from Ref. [107], © The Author(s) 2019.

Table 1 Summary of the conducted LIPSS studies with the type of texture and structural dimensions (periodicity and depth) leading the maximum increase of friction.

Material	Type of texture	Periodicity (nm)	Depth (nm)	Tribological testing	Sliding direction	Friction increase factor	Reference
Crystalline silicon	Periodic grooves	750	150 ± 50	Ball-on-disk	Perpendicular to LIPSS	Max. 1.6	[106]
100Cr6 steel	Periodic grooves	900	200 ± 30	Ball-on-disk	Perpendicular to LIPSS	Max. 4	[107]
CoCrMo alloy	Single- and multi-scale grooves	800		Ball-on-disk	Perpendicular to LIPSS	Max. 3	[108]
⟨111⟩ single crystal silicon (p-doped)	Periodic grooves	730	230	Ball-on-disk	Perpendicular to LIPSS	Max. 3.5	[109]

Apart from LIPSS, Wang et al. [110] fabricated micro-grooves with variable periodicity by femtosecond laser processing in steel, while keeping the groove width and depth constant. Compared to the untreated reference, the COF increased for small groove periodicities (15 and 25 μm) before showing a decreasing tendency with substantially lower COF values for spacings larger than 50 μm. The increased COF for the smallest periods was correlated with a reduced ability to store produced wear debris and an enlarged contact area due to the contact with more individual grooves.

Dunn et al. [100] investigated to possibility to generate high friction surfaces (COF > 0.6) on steel by pursuing different texturing strategies thus varying pulse overlap and pulse energy (Fig. 3(a)). To verify the effect of the produced surface texturing on the resulting static friction, the specimens were clamped into a hydraulic press and friction was measured when applied a normal load to induce motion. While the static COF for the untreated reference was about 0.22, surface texturing increased the static COF irrespective of the used pulse energy and pulse overlap. The greatest increase in friction was observed for a pulse energy of 0.8 mJ and overlaps between 50 and 95% thus leading to an increase by a factor of 4 (Fig. 3(b)). A detailed study of the resulting surface hardness after surface texturing also verified a 1.5-fold increase of the resulting hardness, which was mainly traced back to the formation of oxides. The authors demonstrated that the increase in static friction correlated well with the resulting surface hardness.

Schille et al. [111] laser-textured 42CrMo4 steel surfaces with hemispherical textures and deep welding dots using q-switched nanosecond and continuous wave (CW) laser processing, respectively. Hemispherical dimples (Fig. 4(a)) increased the resulting frictional torque by a factor of 1.8. This has been validated by a shaft-hub connection as a first real-life technical application (Fig. 4(b)) [111]. For welding dots with diameter of 330 μm and height of 70 μm (Fig. 4(c)), a maximum kinetic COF of about 0.8 was verified,

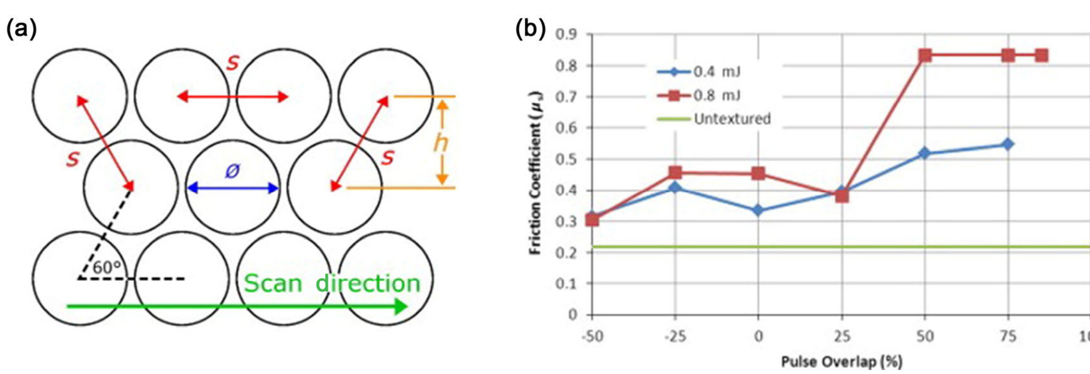

Fig. 3 (a) Texturing strategy with variable pulse overlap and pulse energy. (b) Resulting COF versus pulse overlap for nanosecond laser pulses of 0.4 and 0.8 mJ optical energy irradiated to steel, respectively. Reproduced with permission from Ref. [100], © The Author(s) 2014.

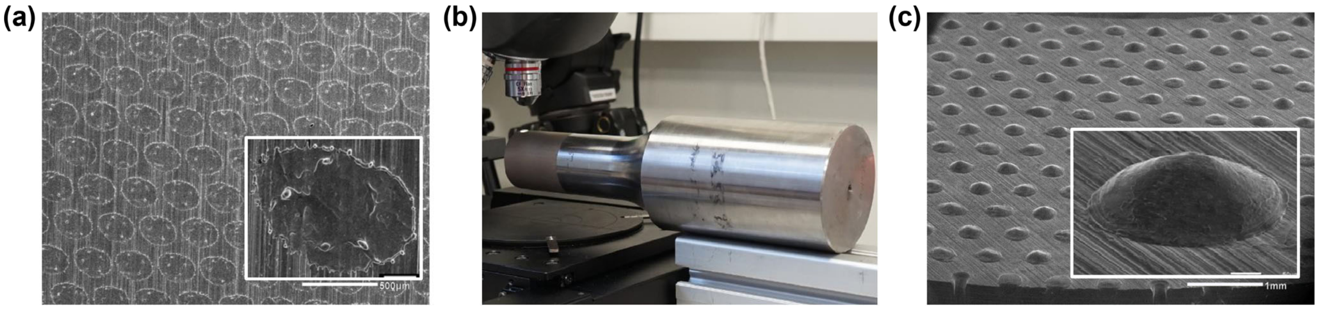

Fig. 4 (a) Hemispherical textures made by ns-pulsed LST; (b) hemispherical textures on a shaft-hub connection; (c) deep-welding dots produced by CW laser irradiations. Reproduced with permission from Ref. [111], © The Author(s) 2015.

which represented an increase by a factor of 2.

Regarding lubricated, non-conformal point contacts, Joshi et al. [112] studied hemispherical dimples in hexagonal and triangular arrangement as well as rectangular structures in stainless steel (1.4112). When properly matching the contact/working conditions with the lateral textures' dimensions, surface textures were capable to tune the resulting frictional performance under boundary and mixed lubrication, thus intentionally increasing or decreasing friction, depending on the adjusted area density. For the precise adjustment of the resulting frictional properties, they identified two competing factors. On the one hand, surface textures may induce pronounced edge effects and stress raisers, thus increasing wear and, therefore, friction. On the other hand, surface textures help to store produced wear debris, thus removing it from the tribological contact zone and reducing abrasion.

3.2 Surface texturing for increased adhesion

Animals such as insects, spiders, and lizards have the surfaces of their attachment pads covered by fine patterns of protuberances. Their remarkable adhesion has been inspiring the development of artificially textured polymers with super-adhesive characteristics. The working principle is based on the idea of contact splitting, creating a large number of small contacts rather than a small number of large contacts [113].

To understand this working principle, Arzt et al. [114] have proposed that the terminations of the setose or hairy systems could be considered hemispherical to use the Hertzian theory to estimate the diameter of the contact area. Including surface attraction effects in the Hertzian theory, Johnson et al. [79], predicted a finite pull-off force between a hemispherical tip and a flat contacting surface (P_c) as

$$P_c = \frac{3}{2}\pi R\gamma \tag{1}$$

for which R is the radius of the hemispherical tip and γ is the adhesion energy per area.

Animals take advantage of the fact that the adhesion force is proportional to a linear dimension of the contact in Eq. (1) [114]. This means that by splitting up the contact into n smaller contacts (setae), each with radius equals to $\sqrt{n}R$, the total adhesion force increases to

$$P_c' = \sqrt{n}P_c \tag{2}$$

For geckos, the surface structure is hierarchical and highly anisotropic. The setose structures are relatively hard (β-keratin, E ~ 1–2 GPa), combined with compliant pads. This combination enables intimate contact of the setae and spatula pads with opposing surfaces, maximizing the weak van der Waals forces, thus adhesion and friction [115]. Similarly, newts can also move on wet and almost vertical glass surface without slipping. Their hierarchical surface structure consists of polygonal cells (30 μm) separated by narrow grooves (0.5 μm), where each cell contains much smaller hemispheric bulges (300 nm) and channels [116]. Tree frogs also show a similar hierarchical structure of hexagonal cells with arrays of nanopillars (300–400 nm), separated by channels filled with mucous [117]. It is believed that an additional mechanism that allows high friction under wet conditions involves the liquid stored in the channels, forming capillary bridges that increase adhesion [116]. Moreover, the channels enable a draining effect by expelling the fluid out of the contact layer to achieve high frictional forces. Finally, chemical components present in the secretions emitted by frogs may play a role on their friction [117].

Inspired by nature, surface texturing has been used in many engineering applications to create high-adhesion biomimetic surfaces. For biomimetic compliant surfaces, instead of laser texturing, the main technique involves producing a patterned mold (often a silicon wafer) by photolithography, where a polymeric resin is poured and then cured to form a textured compliant surface.

Using the concept of contact splitting, elastomeric surfaces were patterned with micropillars of different shapes and dimensions. The adhesion of the patterned polymers was assessed from load-displacement curves obtained from instrumented indentation tests using a spherical sapphire tip (Fig. 5). Comparing pillars with flat, spherical, concave, mushroom-type, and spatular tips, the pull-off force (P_c') of spatular (Fig. 5(c)) and mushroom-like (Fig. 5(d)) patterns was 30 times higher than for the untextured surface (P_c). However,

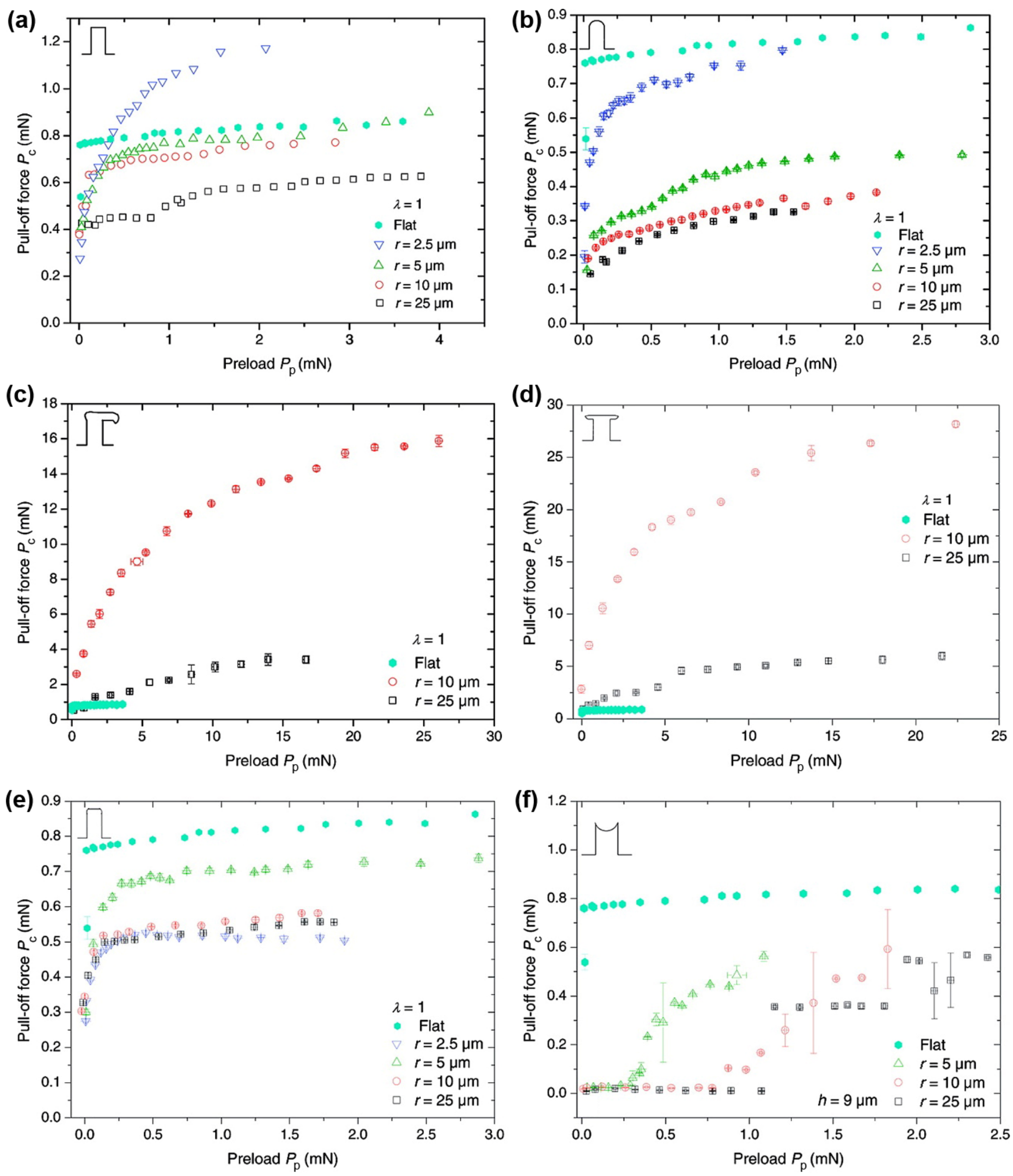

Fig. 5 Effects of surface texturing on pull-off force for different texture patterns: (a) flat pillars; (b) spherical pillars; (c) spatular pillars; (d) mushroom-like pillars; (e) flat with round edges; (f) concave pillars. Reproduced with permission from Ref. [113], © American Chemical Society 2007.

for spherical (Fig. 5(b)), rounded edge (Fig. 5(e)) and concave (Fig. 5(f)) tips, P_c' was lower than P_c, which was attributed to the loss of real contact area in the patterned cases, which probably could not be compensated by the increase in adhesion force due to contact splitting [113].

Jin et al. [115] used a patterned silicon mold to create an inverse polydimethylsiloxane (PDMS) replica, where then polyurethane (PU) was poured to fabricate a two-level hierarchical PU-based dry adhesive with biomimetic gecko-like surface structure. In experimental measurements against a glass surface, they found high friction and adhesion forces in the gripping direction, attributed to the large contact area generated between the adhesive pads and the glass surface [115]. A similar approach was used to produce newt-like surface structures in PDMS. Pin-on-disk tests showed an increase in friction force superior to one order of magnitude [116].

Besides soft compliant surfaces, rigid surfaces have also been textured to increase their adhesion. Kang et al. [118] systematically investigated the resulting adhesional and friction behavior of micro- and nano-textured aluminum surfaces compared to a smooth reference substrate. In this context, micro-dome textures with diameter and height of 3 and 1.5 μm, respectively, were fabricated using a polymer reflow technique coupled with an etching process, while the nano-textures (diameter of 250 nm) were generated by anodic aluminum oxidation. For dry conditions, the micro- and nano-textures demonstrated an increased work of adhesion, which also induced a notably increased COF. The greatest effect was verified for the nano-textured samples with an increase by a factor of 2.7.

Another important point regarding the control of adhesion by surface texturing is the true area of contact since the strength of van-der-Waals forces greatly decreases when the distance between the surfaces increases. Although the surface area increases with surface texturing, more elastic strain energy is needed for the adhesion structure to conform to the texture, making contact. Only very compliant materials can adhere well on hard rough surfaces, since the energy stored during elastic deformation is low compared to the energy gained by forming a contact. The work of adhesion should control attachment and detachment. Cañas et al. [119] have proposed design guidelines for surface texturing to increase adhesion depending on the material´s physical and mechanical properties. For a textured rigid surface in contact with a flat compliant surface, dimples should be shallow and small to promote intimate contact of the adhering surfaces thus increasing adhesion. If the dimple is deep and large and the deformable surface is rigid, a gap will be formed between both surfaces, reducing adhesion [119].

Bonding between surfaces can also be improved by increasing the real contact area. Textured bonded joints have gained increased attention. Laser texturing has been used in bonded joints made in carbon fiber reinforced polymers (CFRP) and epoxy adhesive. Dimples were laser textured on the adherend surfaces for area coverages of 13%, 20%, and 35%, and adherence was evaluated using end-notched flexure tests. Untextured specimens showed unstable crack propagation, while texturing improved the tackiness of the substrate with the adhesive used. The highest bonding resistance was observed for laser treated surfaces of 13% area coverage [120].

The mechanism of interlocking between surface irregularities can also improve bonding between surfaces [121]. Laser texturing of an aluminum alloy improved bonding with a polymeric surface during friction stir welding, producing joints with higher resistance. The bonding mechanism caused by the textured grooves was attributed to mechanical interlocking [122]. A similar mechanism of mechanical interlocking with surface texturing has been proposed for other joining techniques and materials, such as adhesive bonding of PEEK-carbon fiber composites [123], and hot-pressing joining of carbon fiber reinforced polymers with titanium alloys [124].

Surface texturing can also help the bonding between a coating and the substrate via a variety of mechanisms, since texturing increases the true area of contact, raises the substrate's surface energy, and reduces property gradient between substrate and coating. For instance, for a bilayer coating of soft WS_2 coating deposited onto a hard TiAlN coating, plasma-assisted laser texturing of the TiAlN surface prior to WS_2 deposition was used and the adhesive strength of WS_2/TiAlN coatings was measured by the critical load to induce peel-off load in scratch tests. Plasma-assisted surface texturing increased the critical load, as well as the coatings' wear life. The authors attributed this improvement to a series of possibly combined mechanisms: (1) high compressive stresses induced on the TiAlN surface helped to inhibit the initiation and propagation of cracks during deposition of the WS_2 coating; (2) the increase in surface energy with surface texturing triggered covalent chemical bonds between TiAlN and the subsequent WS_2 coating, increasing adhesion; and (3) during deposition, capillary condensation adsorption occurred in the textures, improving adsorption capacity and thus benefitting coating nucleation [125]. For hard DLC coating onto a soft carbon steel substrate, laser texturing using different textures were used prior to deposition of a multilayer Cr/CrN/DLC film, improving adhesion measured by scratch tests. It was hypothesized that laser texturing hindered the continuous propagation of cracks due to stress release during the DLC deposition. Moreover, the resulting wear tracks were smoother for the textured DLC compared to the untextured DLC, with debris filling the textures [126]. However, for DLC deposition onto much softer poly-ether-ether-ketone (PEEK), laser texturing did not improve the adhesion between the DLC coating and the PEEK substrate, probably because the differences in mechanical properties between the coating and the substrate were too large and could not be alleviated by surface texturing [127].

3.3 Surface texturing of systems for movement transmission and control

Increase of friction can be fundamental to control some mechanical transmission systems such as ultrasonic motors (USMs) and continuously variable transmissions (CVTs), opening an important route for the use surface texturing as a technique to improve the performance of such systems. USMs use the reverse piezoelectric effect to drive the stator vibration in the ultrasonic frequency band. Under the action of an electric field, the stator surface experiences an elliptical movement, but if a normal load is applied to the rotor, frictional force transforms the elliptical motion into rotary motion. Therefore, the COF dictates the output torque of USMs. Liu et al. [128] used nanosecond laser texturing to produce different textures on polyimide plates used as friction material in USMs. They verified the highest COF for dimples with a diameter of 300 μm and area coverage of around 7%. Moreover, the untextured polyimide surfaces showed severe abrasive wear, which was not observed with texturing, attributed to the entrapment of wear debris within the textures. In another work, they measured the rotational speed and output power of the USMs using textured and untextured friction plates [128]. The rotational speed of the USM was higher (faster motor) for the textured than for the untextured plates and a clear improvement in the output torque was observed with surface texturing [128].

Surface texturing can also affect the performance of CVTs. CVTs transmit torque between two sets of conical pulleys by means of friction between a metal push-belt and the pulley surface. On the one hand, reducing friction losses at the belt-pulley contact improves the CVT efficiency. On the other hand, high circumferential frictional forces on the pulleys are needed for good torque transmission efficiency. This implies that different frictional characteristics are required in different directions. The use of surface texturing has been proposed to create friction anisotropy at the belt-pulley contact in CVT systems. The generation of friction anisotropy by surface texturing could potentially optimize friction characteristics of the belt/pulley contact. To investigate this aspect, different laser textures were tested in four different directions under lubricated conditions. Friction anisotropy was observed for textures with parallel grooves and dotted-line grooves, with highest friction in the direction parallel to the grooves, which gradually decreased until the sliding direction was perpendicular to the grooves. It was hypothesized that for groove-type textures both the lubricant supply and the amount of plateaus for contact vary with the sliding direction [129].

For systems that rely on high friction to control the movement between surfaces such as clutches and brakes, surface texturing has also been explored. Braking performance of textured braking discs using magnetorheological fluid brake has been investigated in a specially-designed prototype. Dimples produced by laser texturing increased the friction coefficient of a brake system, as well as helped to resist the heat fade phenomenon by reducing the interface temperature of the brake disc [130].

Another example of laser texturing increasing the efficiency of mechanical systems for movement control involves solar panels of a space satellite. During integration, the solar panel is fixed close to the satellite body in its closed position using a locking system and surface texturing could help interlocking. This was achieved by deep laser-textured grooves. On the other hand, during deployment, the panel must be able to slip open, but a textured surface would stick. To overcome this, the textured surface was subsequently coated with DLC, to prevent the occurrence of cold welding. However, it needs to be pointed out that the COF was measured only in a static condition [131].

3.4 Friction anisotropy in biomimetic applications

In many biological systems, evolution has developed surfaces with anisotropic friction where COFs depending on the sliding direction enable complex functionalities. Inspired by such systems, mechanical systems for which surface texturing could lead to anisotropic friction have been widely proposed and investigated in recent years. For instance, anisotropic friction enables limbless motion in snakes and could be used to help developing locomotion systems such as snake-type soft robots [132]. Sánchez et al. [133] performed a thorough characterization of snake skins in terms of chemical composition, surface morphology and topography, mechanical properties, and friction. The outer skin was found to be rigid with anisotropic surface morphology, on a significantly more compliant inner skin. When dry friction of the snake skin was measured by pin-on-disc tests against balsa wood in two opposing directions (head-to-tail and tail-to-head), anisotropic friction was identified. Friction in the head-to-tail direction was lower than in the tail-to-head direction since interlocking with the fibrils of the skin was more significant in that direction. Then, the authors textured AISI 52100 specimens with patterns miming the texture the snake skin, consisting of rather elongated elliptical dimples, also finding anisotropic friction [133].

In bio-implants, bioinspired hierarchical morphologies have been used for titanium alloy screws, aiming to reduce friction when screwing in and increasing friction when screwing out. In this regard, laser texturing was used to produce patterns consisting of stacked rings to reduce friction along the stacked ring direction and increase it in the other directions. The hierarchical morphology is presented in Fig. 6(a) and the different relative sliding directions are schematized in Fig. 6(b). For lubricated experiments using simulated body fluids, the COF was found to be reduced in the stacked ring direction (0.20) when compared with an untextured surface (0.24), while friction increased in the other directions, achieving 0.34 in the direction perpendicular to the stacked rings (Fig. 6(c)) [134]. During *in-vitro* tests, the stacked rings provided more sites for apatite deposition, improving the friction stability of the implant surface [135]. The observed effects were traced back to different aspects involving the respective surface topography/roughness, which modifies the textures' ability to store wear debris as well as tailors the real area of contact. In case of the textures with micro-bulges, the existence of the micro-

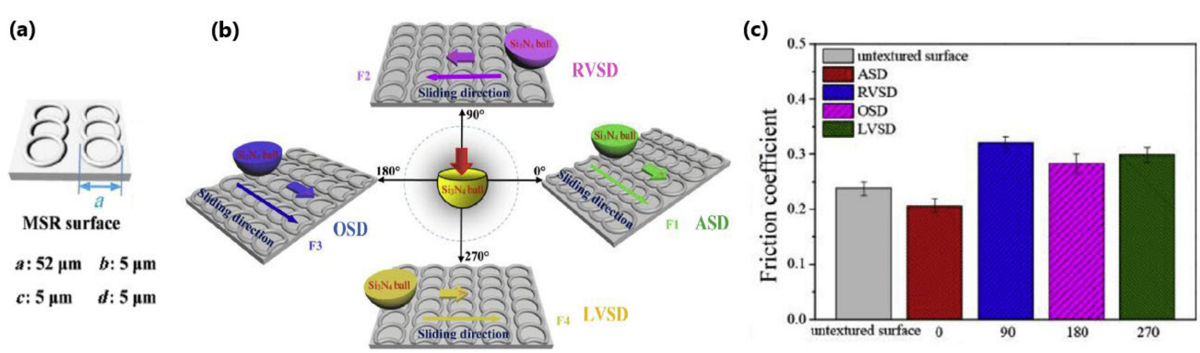

Fig. 6 Analysis of friction anisotropy under lubricated sliding using a simulated body fluid: (a) pattern of the hierarchical texture; (b) sliding directions; (c) average friction results. Reproduced with permission from Ref. [134], © Elsevier Ltd. 2019.

bulges notably reduced the real area of contact thus increasing the coefficient of friction. However, the ring-like texture effectively stored the produced wear debris, which helped to lower wear thus enabling to combine high friction with low wear.

3.5 Surface texturing of the road/tire system

In the road/tire system, skid resistance is a key issue to ensure human safety since the risk of overrun increases tenfold when the road is covered by water. The importance of friction control and measurement in the road/tire system has been under focus for over 60 years. For instance, in runways for aircraft landing, friction measuring devices positioned in the ground devices are used by pilots to estimate the landing distance of the aircraft [136].

Under wet conditions, friction between tire and road can be divided in two components. The first is the adhesion in the localized regions where dry contact occurs. The second is the deformation component at the surface of the tire tread in contact with the hard asperities on the road surface. The relative contribution of each component depends on the interaction between the topographic features of both the tire and road. Moreover, the effectiveness of the adhesion component depends on how the water is drained by through the topographies of the tire and road [137].

Therefore, surface texturing can be used to control the topography and thus friction from both the tire and the road perspective. Regarding the tire topography, the tire tread can be represented as a series of elastic brush elements. The tire/road contact can be decomposed into an adhesion zone and a sliding zone. The water in front of the tire creates a hydrodynamic force that lifts the tire from the road, reducing the adhesion region [136]. Tread grooves in the tire favor water drainage and provide space for temporary water storage, increasing the tire/road-ground contact to improve gripping and skid resistance [138]. Many different groove patterns have been proposed to optimize the tire topography, such as honeycomb patterns [139] and V-shaped groove patterns [140]. More recently, Mao et al. [138] have proposed the use of patterns containing convex hull in different spatial arrangements. To achieve this morphology, they used two types of tire tread compounds with different wear resistances (Ax and By, Fig. 7(a)), so that convex hulls of tire tread were naturally formed after abrasion of the tires. The spatial arrangements of the harder treads varied forming triangles, squares, pentagons, and hexagons. Therefore, the tire had a hierarchical morphology, consisting of both grooves and the convex-hull morphology (Fig. 7(b)). Under wet conditions, the hierarchical surface with convex hull morphology increased the surface roughness, COF and skid resistance when compared with tires only presenting conventional grooves [138].

Regarding the road topography, concrete tends to exhibit low adhesion since it is rigid and often too smooth and compact, therefore presenting low skid resistance. Different textures can have significant impact on the skid resistance of roads since they affect the adhesion coefficient between the tire and the pavement surface. The wet resistance of roads with four types of grooves was measured: transverse

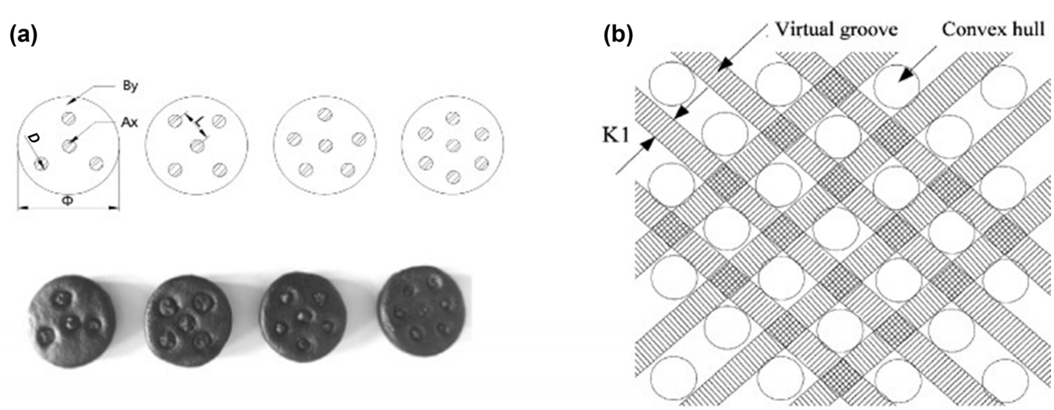

Fig. 7 Hierarchical texture in tires: (a) arrangement of treads with different mechanical properties to form convex hulls; (b) patterns with arrangement of convex hulls and grooves. Reproduced with permission from Ref. [138], © John Wiley & Sons, Inc. 2021.

equidistant grooves, longitudinal equidistant grooves, transverse unequal spacing grooves, and longitudinal and transverse combined grooves. The evaluation consisted of measurements of sideway force coefficient and road roughness in actual roads inside tunnels. Among all the groove textures, longitudinal equidistant grooves for groove width and depth of 5 mm and spacing of 250 mm resulted in the highest wet resistance [141]. Gerthoffert et al. [136] used an IMAG (Instrument de Mesure Automatique de Glissance) to obtain COF values in real roads. In this regard, the force required to tow a braked and loaded wheel at a constant speed measured the friction force at the tire/road interface. COF values were measured under wet conditions for seven surfaces with different characteristics in terms of macro-texture (types of asphalt)- and micro-texture (paint containing glass beads of different average sizes). The road with the roughest micro-texture showed the highest friction. They also developed an analytical model to estimate friction at the tire/road contact, by representing the tire tread as a series of elastic brush elements. The forces acting on each brush element were considered as an elastic force in the adhesion zone or a friction force in the sliding zone. Under wet conditions, the hydrodynamic force reduced the length of the tire/runway contact area, but this effect was reduced by the micro-texture. Very good agreement was found between their model and experiments, reinforcing the proposed mechanism [136]. When the road surface texture is deteriorated by wear, skid resistance has been shown to drastically reduce [142].

In metro railways, the rubber tire rolls over a steel track. Different macro textures have been produced on a steel track. A laboratory pendulum friction tester measured higher friction for the tracks containing grooves than a smooth track, which was attributed to water channeling out on both sides of the steel track [143].

4 Current short-comings, future research directions, and concluding remarks

An overview of the use of surface texturing to intentionally increase friction has been presented. Although surface texturing has been one of the most investigated areas in the last few decades (61,342 documents found for "surface texturing" in Web of Science), the aim of the technique in tribological applications is almost always to reduce friction. The number of works found for friction increase due to surface texturing reported as a desired feature was only 62. Despite this, the vast majority of the works measuring friction of textured surfaces report at least some condition where friction increased with surface texturing. Although they were treated as unwanted conditions, they have shaped the framework for the design of high-friction functional surfaces. This review identified some main areas that have benefitted from high-friction surfaces produced by surface texturing: high-performance adhesives [113, 114, 119] composite bonding [120, 123], adhesion of coatings [125–127], friction welding [122], bioimplants [108, 134, 135], manufacturing [105, 121, 124], mechanical transmission systems [128, 129], brakes [130], movement control [131, 133], robotics [132], and the road-tire contact [136–143].

Although many strategies have been used to produce surface textures for increased friction, laser texturing was by far the most used technique. This review identified the main current trends in laser texturing. The use of USP laser systems is an important route to reduce the thermal impact on the substrates, reducing melting at the microscale to negligible levels. Alternatives to USP lasers at cheaper investment costs are ns-pulsed and continuous wave, which can supply high laser powers in a more cost-efficient manner. To produce sub-micrometric textures, laser induced periodical surface structures (LIPSS) have been shown to be a fast and efficient approach for increasing COF′s at lower loads. A recent innovation involves the combination of diffractive optical elements for multi-beams with ultrafast scanning systems, consolidating high-rate LST as a key technology in modern surface engineering.

Other applications can be envisaged for high-friction textured surfaces, such as clutches and sensory systems. When a surface is touched, surface textures have a crucial effect on tactile perception, mainly due to differences in friction between the finger and the surface, as well as the deformation of the skin [144]. The penetration of the fingertip between raised texture elements, and the respective interlocking with these elements, among other phenomena, govern tactile perception [145]. When an object is manipulated, the generated forces provide sensory cues for the nervous system, enabling the qualities of the object's surface to be identified [146]. Therefore, a frictional increase may help either the development of artificial sensors to implement artificial haptic systems, including reality-augmented haptic systems [147] or the design of artificial surfaces that can mimic the human feel of natural surfaces. This area has been identified as a hotspot with large research potential for high-friction textured surfaces [20].

The ability to tune friction to higher or lower values is another emerging topic. This has been proved possible for directional textures, where friction can be low in one direction and high in another direction, giving different functionalities to components such as implants [134, 135] and robots [132]. However, one fairly unexplored path is anisotropic friction depending on operational conditions, where friction for textured surfaces could be higher or lower depending on conditions such as load, speed, temperature and environment, thus creating smart textured surfaces.

The main mechanisms involved in friction increase due to surface texturing related to the increase in the real contact area [110, 118, 135], particularly when at least one of the surfaces was compliant [119, 120, 136], to contact splitting [113, 114], to the increase of the deformation component of friction [106, 109], to mechanical interlocking [121–124, 131], to stress concentration with possible micro-cutting at the texture edges [105, 112], to changes in surface chemistry [106, 125], to tribo-chemical surface reactions [100, 109], to surficial phase transitions [106], to stress release [126] or the induction of compressive stresses in coated systems [125], to an increase of deposition nucleation rate [125, 135], and to water channeling for skid resistance [136–143]. An important feature found in many works was that although surface texturing increased friction, the surfaces did not necessarily show more wear. This was mostly attributed to the removal of wear debris from the contact by the textures [48, 105, 112, 128, 135]. In some works, more efficient heat transfer with textures helped to reduce wear [108, 130].

It is worth pointing out that most of the work found was experimental, often using trial-and-error approaches. In order to optimize functionalization of high-friction surfaces via surface texturing, analytical and numerical modelling approaches are urgently needed. Numerical modelling has already been successfully used to predict the tribological performance of surface textures under hydrodynamic [57, 70, 68, 69, 148, 149] and elastohydrodynamic conditions [150–154]. Significant research progress has been also made related to the numerical prediction of mixed lubrication [59, 155, 156]. In this regard, we anticipate that similar approaches can be used to predict the behavior of surface textures with the overall aim to intentionally increase friction. Another approach with great potential in this area involves machine learning techniques, particularly in areas that already have a substantial amount of data, such as the tire-road system, bioimplants and brake systems.

Acknowledgements

This work was supported by ANID-CONICYT within the project Fondecyt 11180121 and Fondequip EQM190057 as well as the VID of the University of Chile in the framework of "U-Inicia UI013/2018". HLC acknowledges financial support from Fapergs/Brazil (No. 19/2551-0001849-5) and CNPq/Brazil (No. 305453/2017-3). JS thanks the German Federal Ministry of Education and Research (BMBF) for financial support in the project FH-Europa 2020: MACH-XLT (No. 13FH009EX0).

References

[1] Shah R, Woydt M, Huq N, Rosenkranz A. Tribology meets sustainability. *Ind Lubr Tribol* **73**(3): 430–435 (2021)

[2] Taylor RI. Tribology and energy efficiency: From molecules to lubricated contacts to complete machines. *Faraday Discuss* **156**: 361–382 (2012)

[3] Holmberg K, Erdemir A. The impact of tribology on energy use and CO_2 emission globally and in combustion engine and electric cars. *Tribol Int* **135:** 389–396 (2019)

[4] Holmberg K, Erdemir A. Influence of tribology on global energy consumption, costs and emissions. *Friction* **5**(3): 263–284 (2017)

[5] John S, El-Ghoul Z, Dimkovski Z, Lööf P J, Lundmark J, Mohlin J. Friction between pin and roller of a truck's valvetrain. *Surf Topogr*: *Metrol Prop* **7**(1): 014001 (2019)

[6] Ballam M H, Karimzadeh F, Enayati M H, Sanati A. Developing a nanostructured surface layer on AISI 316 stainless steel by ultrasonic surface nanocrystallization and evaluating its tribological properties. *Surf Topogr*: *Metrol Prop* **9**(2): 025010 (2021)

[7] He J Q, Sun J L, Meng Y N, Yan X D. Preliminary investigations on the tribological performance of hexagonal boron nitride nanofluids as lubricant for steel/steel friction pairs. *Surf Topogr*: *Metrol Prop* **7**(1): 015022 (2019)

[8] Patel P R, Sharma S, Tiwari S K. Tribological properties of aluminium reinforced with differently oriented carbon nanotube: A molecular dynamics study. *Surf Topogr*: *Metrol Prop* **9**(2): 025035 (2021)

[9] Morais R R Jr, Cardoso G V, Ferreira E S, Costa H L. Surface characterization, mechanical and abrasion resistance of nanocellulose-reinforced wood panels. *Surf Topogr*: *Metrol Prop* **8**(2): 025011 (2020)

[10] Katta J, Jin Z M, Ingham E, Fisher J. Biotribology of articular cartilage—A review of the recent advances. *Med Eng Phys* **30**(10): 1349–1363 (2008)

[11] Gebeshuber I C. Biotribology inspires new technologies. *Nano Today* **2**(5): 30–37 (2007)

[12] Meng Y G, Xu J, Jin Z M, Prakash B, Hu Y Z. A review of recent advances in tribology. *Friction* **8**(2): 221–300 (2020)

[13] Austin R S, Mullen F, Bartlett D W. Surface texture measurement for dental wear applications. *Surf Topogr*: *Metrol Prop* **3**(2): 023002 (2015)

[14] Richard C. Lipstick adhesion measurement. In *Surface Science and Adhesion in Cosmetics*. Mittal K, Bui H, eds. Wiley, 2021: 635–662.

[15] Bui H S, Coleman-Nally D. Film-forming technology and skin adhesion in long-wear cosmetics. In *Adhesion in Pharmaceutical, Biomedical and Dental Fields.* Mittal K, Etzler F, eds. Hoboken (USA): John Wiley & Sons, Inc., 2017: 141–166.

[16] Sterner O, Aeschlimann R, Zürcher S, Scales C, Riederer D, Spencer N D, Tosatti S G P. Tribological classification of contact lenses: From coefficient of friction to sliding work. *Tribol Lett* **63**(1): 1–13 (2016)

[17] Roba M, Duncan E G, Hill G A, Spencer N D, Tosatti S G P. Friction measurements on contact lenses in their operating environment. *Tribol Lett* **44**(3): 387–397 (2011)

[18] Whitehouse S, Myant C, Cann P M, Stephens A. Fluorescent imaging of razor cartridge/skin lubrication. *Surf Topogr*: *Metrol Prop* **9**(2): 024001 (2021)

[19] Neumann A, Frank D, Vondenhoff T, Schmitt R. Comparison of two metrological approaches for the prediction of human haptic perception. *Surf Topogr*: *Metrol Prop* **4**(2): 025004 (2016)

[20] Sergachev D, Matthews D, van der Heide E. Design of bidirectional frictional behaviour for tactile contact using ellipsoidal asperity micro-textures. *Friction* **10**(5): 762–771 (2022)

[21] Marian M, Shah R, Gashi B, Zhang S, Bhavnani K, Wartzack S, Rosenkranz A. Exploring the lubrication mechanisms of synovial fluids for joint longevity—A perspective. *Colloids Surf B Biointerfaces* **206**: 111926 (2021)

[22] Popov V L, Poliakov A M, Pakhaliuk V I. Synovial joints. tribology, regeneration, regenerative rehabilitation and arthroplasty. *Lubricants* **9**(2): 15 (2021)

[23] Meenakshi C V R, Kumar K S, Ramana S V. Tribological aspects on human knee joint - AReview. *Mater Today Proc* **22**: 3100–3105 (2020)

[24] Link JM, Salinas EY, Hu JC, Athanasiou KA. The tribology of cartilage: Mechanisms, experimental techniques, and relevance to translational tissue engineering. *Clin Biomech* (*Bristol*, *Avon*) **79**: 104880 (2020)

[25] Laguna L, Sarkar A. Oral tribology: Update on the relevance to study astringency in wines. *Tribol Mater Surf Interfaces* **11**(2): 116–123 (2017)

[26] Sarkar A, Krop E M. Marrying oral tribology to sensory perception: A systematic review. *Curr Opin Food Sci* **27**: 64–73 (2019)

[27] Upadhyay R, Chen J S. Smoothness as a tactile percept: Correlating 'oral' tribology with sensory measurements. *Food Hydrocoll* **87**: 38–47 (2019)

[28] Strey N F, Scandian C. Tribological transitions during sliding of zirconia against alumina and ZTA in water. *Wear* **376–377**: 343–351 (2017)

[29] Balarini R, Strey N F, Sinatora A, Scandian C. The influence of initial roughness and circular axial Run-out on friction and wear behavior of Si_3N_4–Al_2O_3 sliding in water. *Tribol Int* **101**: 226–233 (2016)

[30] Wang X D, Sato H, Adachi K. Low friction in self-mated silicon carbide tribosystem using nanodiamond as lubricating additive in water. *Friction* **9**(3): 598–611 (2021)

[31] Donato M T, Colaço R, Branco L C, Saramago B. A review on alternative lubricants: Ionic liquids as additives and deep eutectic solvents. *J Mol Liq* **333**: 116004 (2021)

[32] Seed C M, Acharya B, Krim J. QCM study of tribotronic control in ionic liquids and nanoparticle suspensions. *Tribol Lett* **69**(3): 1–12 (2021)

[33] Spikes H. The history and mechanisms of ZDDP. *Tribol Lett* **17**(3): 469–489 (2004)

[34] Spikes H. Friction modifier additives. *Tribol Lett* **60**(1): 1–26 (2015)

[35] Dias H W J, Medeiros A B, Binder C, Rodrigue Neto J B, Klein A N, de Mello J D B. Tribological evaluation of turbostratic 2D graphite as oil additive. *Lubricants* **9**(4): 43 (2021)

[36] Furlan K P, de Mello J D B, Klein A N. Self-lubricating composites containing MoS_2: A review. *Tribol Int* **120**: 280–298 (2018)

[37] Scharf T W, Prasad S V. Solid lubricants: A review. *J Mater Sci* **48**(2): 511–531 (2013)

[38] Grützmacher P G, Suarez S, Tolosa A, Gachot C, Song G C, Wang B, Presser V, Mücklich F, Anasori B, Rosenkranz A. Superior wear-resistance of Ti3C2Tx multilayer coatings. *ACS Nano* **15**(5): 8216–8224 (2021)

[39] Wyatt B C, Rosenkranz A, Anasori B. 2D MXenes: Tunable mechanical and tribological properties. *Adv Mater* **33**(17): 2007973 (2021)

[40] Tavares A F, Lopes A P O, Mesquita E A, Almeida D T, Souza J H C, Costa H L. Effect of transfer layers on friction and wear mechanisms in strip drawing tests of commercially coated forming tools. *Wear* **476**: 203733 (2021)

[41] Hamilton D B, Walowit J A, Allen C M. A theory of lubrication by microirregularities. *J Basic Eng* **88**(1): 177–185 (1966)

[42] Anno J N, Walowit J A, Allen C M. Load support and leakage from microasperity-lubricated face seals. *J Lubr Technol* **91**(4): 726–731 (1969)

[43] Etsion I. State of the art in laser surface texturing. *J Tribol* **127**(1): 248–253 (2005)

[44] Rapoport L, Moshkovich A, Perfilyev V, Gedanken A, Koltypin Y, Sominski E, Halperin G, Etsion I. Wear life and adhesion of solid lubricant films on laser-textured steel surfaces. *Wear* **267**(5–8): 1203–1207 (2009)

[45] Shinkarenko A, Kligerman Y, Etsion I. Theoretical analysis of surface-textured elastomer sleeve in lubricated rotary sliding. *Tribol Trans* **53**(3): 376–385 (2010)

[46] Rosenkranz A, Reinert L, Gachot C, Mücklich F. Alignment and wear debris effects between laser-patterned steel surfaces under dry sliding conditions. *Wear* **318**(1–2): 49–61 (2014)

[47] Shimizu J, Nakayama T, Watanabe K, Yamamoto T, Onuki T, Ojima H, Zhou L B. Friction characteristics of mechanically microtextured metal surface in dry sliding. *Tribol Int* **149**: 105634 (2020)

[48] Rodrigues T A, Arencibia R V, Costa H L, da Silva W M. Roughness analysis of electrochemically textured surfaces: Effects on friction and wear of lubricated contacts. *Surf Topogr*: *Metrol Prop* **8**(2): 024011 (2020)

[49] da Silva L R R, Costa H L. Tribological behavior of gray cast iron textured by maskless electrochemical texturing. *Wear* **376–377**: 1601–1610 (2017)

[50] Braun D, Greiner C, Schneider J, Gumbsch P. Efficiency of laser surface texturing in the reduction of friction under mixed lubrication. *Tribol Int* **77**: 142–147 (2014)

[51] Rosenkranz A, Szurdak A, Gachot C, Hirt G, Mücklich F. Friction reduction under mixed and full film EHL induced by hot micro-coined surface patterns. *Tribol Int* **95**: 290–297 (2016)

[52] Wang X L, Kato K, Adachi K, Aizawa K. The effect of laser texturing of SiC surface on the critical load for the transition of water lubrication mode from hydrodynamic to mixed. *Tribol Int* **34**(10): 703–711 (2001)

[53] Krupka I, Hartl M, Zimmerman M, Houska P, Jang S. Effect of surface texturing on elastohydrodynamically lubricated contact under transient speed conditions. *Tribol Int* **44**(10): 1144–1150 (2011)

[54] Mourier L, Mazuyer D, Ninove F P, Lubrecht A A. Lubrication mechanisms with laser-surface-textured surfaces in elastohydrodynamic regime. *Proc Inst Mech Eng Part J J Eng Tribol* **224**(8): 697–711 (2010)

[55] Choo J W, Glovnea R P, Olver A V, Spikes H A. The effects of three-dimensional model surface roughness features on lubricant film thickness in EHL contacts. *J Tribol* **125**(3): 533–542 (2003)

[56] Costa H L, Hutchings I M. Hydrodynamic lubrication of textured steel surfaces under reciprocating sliding conditions. *Tribol Int* **40**(8): 1227–1238 (2007)

[57] Rosenkranz A, Costa H L, Profito F, Gachot C, Medina S, Dini D. Influence of surface texturing on hydrodynamic friction in plane converging bearings—An experimental and numerical approach. *Tribol Int* **134:** 190–204 (2019)

[58] dos Santos M B, Costa H L, de Mello J D B. Potentiality of triboscopy to monitor friction and wear. *Wear* **332–333**: 1134–1144 (2015)

[59] Gu C X, Meng X H, Xie Y B, Yang Y M. Effects of surface texturing on ring/liner friction under starved lubrication. *Tribol Int* **94**: 591–605 (2016)

[60] Suh N P, Mosleh M, Howard P S. Control of friction. *Wear* **175**(1–2): 151–158 (1994)

[61] Hichri Y, Cerezo V, Do M T, Zahouani H. Effect of particles' characteristics and road surface's texture on the tire/road friction. *Surf Topogr*: *Metrol Prop* **6**(3): 034014 (2018)

[62] Yu A B, Niu W Y, Hong X, He Y, Wu M C, Chen Q J, Ding M L. Influence of tribo-magnetization on wear debris trapping processes of textured dimples. *Tribol Int* **121**: 84–93 (2018)

[63] Zhu Y M, Chen J J, Du J J, Fan Y J, Zheng J F. Tribological behavior of laser textured nodular cast iron surface. *Ind Lubr Tribol* **71**(7): 949–955 (2019)

[64] Pettersson U, Jacobson S. Influence of surface texture on boundary lubricated sliding contacts. *Tribol Int* **36**(11): 857–864 (2003)

[65] Gachot C, Hsu C, Suárez S, Grützmacher P, Rosenkranz A, Stratmann A, Jacobs G. Microstructural and chemical characterization of the tribolayer formation in highly loaded cylindrical roller thrust bearings. *Lubricants* **4**(2): 19 (2016)

[67] Hsu C J, Stratmann A, Medina S, Jacobs G, Mücklich F, Gachot C. Does laser surface texturing really have a negative impact on the fatigue lifetime of mechanical components? *Friction* **9**(6): 1766–1775 (2021)

[68] Olver A V, Fowell M T, Spikes H A, Pegg I G. 'Inlet suction', a load support mechanism in non-convergent, pocketed, hydrodynamic bearings. *Proc Inst Mech Eng Part J J Eng Tribol* **220**(2): 105–108 (2006)

[69] Fowell M, Olver A V, Gosman A D, Spikes H A, Pegg I. Entrainment and inlet suction: Two mechanisms of hydrodynamic lubrication in textured bearings. *J Tribol* **129**(2): 336–347 (2006).

[70] Gropper D, Wang L, Harvey T J. Hydrodynamic lubrication of textured surfaces: A review of modeling techniques and key findings. *Tribol Int* **94**: 509–529 (2016)

[71] Gachot C, Rosenkranz A, Hsu S M, Costa H L. A critical assessment of surface texturing for friction and wear improvement. *Wear* **372–373**: 21–41 (2017)

[72] Rosenkranz A, Grützmacher P G, Gachot C, Costa H L. Surface texturing in machine elements—A critical discussion for rolling and sliding contacts. *Adv Eng Mater* **21**(8): 1900194 (2019)

[73] Rosenkranz A, Costa H L, Baykara M Z, Martini A. Synergetic effects of surface texturing and solid lubricants to tailor friction and wear - A review. *Tribol Int* **155**: 106792 (2021)

[74] Lu P, Wood R J K. Tribological performance of surface texturing in mechanical applications—A review. *Surf Topogr*: *Metrol Prop* **8**(4): 043001 (2020)

[75] Vineeth Kumar V, Senthil Kumaran S. Friction material composite: Types of brake friction material formulations and effects of various ingredients on brake performance—A review. *Mater Res Express* **6**(8): 082005 (2019)

[76] Xiao X M, Yin Y, Bao J S, Lu L J, Feng X J. Review on the friction and wear of brake materials. *Adv Mech Eng* **8**(5): 168781401664730 (2016)

[77] Terleeva O P, Slonova A I, Rogov A B, Matthews A, Yerokhin A. Wear resistant coatings with a high friction coefficient produced by plasma electrolytic oxidation of Al alloys in electrolytes with basalt mineral powder additions. *Materials* **12**(17): 2738 (2019)

[78] Wu J P, Ma B, Li H Y, Ma C N. Friction and wear properties of three different steels against paper-based friction material. *Ind Lubr Tribol* **71**(10): 1206–1212 (2019)

[79] Johnson K L, Kendall K, Roberts A D, Tabor D. Surface energy and the contact of elastic solids. *Proc R Soc Lond A* **324**(1558): 301–313 (1971)

[80] Sutcliffe M P F. Surface finish and friction in cold metal rolling. In *Metal Forming Science and Practice.* Lenard J G, ed. Oxford (UK): Elsevier Science Ltd., 2002: 19–59.

[81] Costa H L, Hutchings I M. Some innovative surface texturing techniques for tribological purposes. *Proc Inst Mech Eng Part J J Eng Tribol* **229**(4): 429–448 (2015)

[82] Martan J, Moskal D, Kučera M. Laser surface texturing with shifted method—Functional surfaces at high speed. *J Laser Appl* **31**(2): 022507 (2019)

[83] Volpe A, Gaudiuso C, Ancona A. Laser fabrication of anti-icing surfaces: A review. *Materials* **13**(24): 5692 (2020)

[84] Luo X, Yao S L, Zhang H J, Cai M Y, Liu W J, Pan R, Chen C H, Wang X M, Wang L N, Zhong M L. Biocompatible nano-ripples structured surfaces induced by femtosecond laser to rebel bacterial colonization and biofilm formation. *Opt Laser Technol* **124**: 105973 (2020)

[85] Shivakoti I, Kibria G, Cep R, Pradhan B B, Sharma A. Laser surface texturing for biomedical applications: A review. *Coatings* **11**(2): 124 (2021)

[86] Schille J, Schneider L, Mauersberger S, Szokup S, Höhn S, Pötschke J, Reiß F, Leidich E, Löschner U. High-rate laser surface texturing for advanced tribological functionality. *Lubricants* **8**(3): 33 (2020)

[87] Sitar A, Crivellari M, Schille J, Mauersberger S, Löschner U, Golobič I. Improved boiling heat transfer in dry etched microchannels with laser structured surfaces. In *ASME 2018 16th International Conference on Nanochannels, Microchannels, and Minichannels*, Dubrovnik, Croatia, 2018: V001T02A015.

[88] Birnbaum M. Semiconductor surface damage produced by ruby lasers. *J Appl Phys* **36**(11): 3688–3689 (1965)

[89] Reif J, Varlamova O, Varlamov S, Bestehorn M. The role of asymmetric excitation in self-organized nanostructure formation upon femtosecond laser ablation. *Appl Phys A* **104**(3): 969–973 (2011)

[90] Bonse J, Höhm S, Kirner S V, Rosenfeld A, Krüger J. Laser-induced periodic surface structures—A scientific evergreen. *IEEE J Sel Top Quantum Electron* **23**(3): 9000615 (2017)

[91] Tsukamoto M, Kayahara T, Nakano H, Hashida M, Katto M, Fujita M, Tanaka M, Abe N. Microstructures formation on titanium plate by femtosecond laser ablation. *J Phys*: *Conf Ser* **59**: 666–669 (2007)

[92] Bruening S, Du K M, Jarczynski M, Gillner A. High-

throughput micromachining with ultrashort pulsed lasers and multiple spots. *J Laser Appl* **32**(1): 012003 (2020)

[93] Gillner A, Finger J, Gretzki P, Niessen M, Bartels T, Reininghaus M. High power laser processing with ultrafast and multi-parallel beams. *J Laser Micro/Nanoengin* **2019**: 218550959 (2019).

[94] Bonse J, Krüger J, Höhm S, Rosenfeld A. Femtosecond laser-induced periodic surface structures. *J Laser Appl* **24**(4): 042006 (2012)

[95] Gregorčič P, Sedlaček M, Podgornik B, Reif J. Formation of laser-induced periodic surface structures (LIPSS) on tool steel by multiple picosecond laser pulses of different polarizations. *Appl Surf Sci* **387**: 698–706 (2016)

[96] Hirsiger T, Gafner M, Remund S M, Chaja M W, Urniezius A, Butkus S, Neuenschwander B. (2020) Machining metals and silicon with GHz bursts: Surprising tremendous reduction of the specific removal rate for surface texturing applications. In *Proceedings Volume 11267 Laser Applications in Microelectronic and Optoelectronic Manufacturing (LAMOM) XXV*, San Francisco, USA, SPIE, 2020: 112670T.

[97] Ackerl N, Fisch G, Auerswald J, Wegener K. Evolution of microstructures on stainless steel induced by ultra-short pulsed laser ablation. *SN Appl Sci* **2**(4): 1–10 (2020)

[98] Gedvilas M, Mikšys J, Račiukaitis G. Flexible periodical micro- and nano-structuring of a stainless steel surface using dual-wavelength double-pulse picosecond laser irradiation. *RSC Adv* **5**(92): 75075–75080 (2015)

[99] Hwang T Y, Guo C L. Angular effects of nanostructure-covered femtosecond laser induced periodic surface structures on metals. *J Appl Phys* **108**(7): 073523 (2010)

[100] Dunn A, Carstensen J V, Wlodarczyk K L, Hansen E B, Gabzdyl J, Harrison P M, Shephard J D, Hand D P. Nanosecond laser texturing for high friction applications. *Opt Lasers Eng* **62**: 9–16 (2014)

[101] Röcker C, Loescher A, Delaigue M, Hönninger C, Mottay E, Graf T, Ahmed M A. Flexible sub-1 ps ultrafast laser exceeding 1 kw of output power for high-throughput surface structuring. In *Laser Congress 2019 (ASSL, LAC, LS&C)*, Vienna, OSA, 2019.

[102] Müller M, Aleshire C, Klenke A, Haddad E, Légaré F, Tünnermann A, Limpert J. 104 kW coherently combined ultrafast fiber laser. *Opt Lett* **45**(11): 3083 (2020)

[103] Schille J, Schneider L, Streek A, Kloetzer S, Loeschner U. High-throughput machining using a high-average power ultrashort pulse laser and high-speed polygon scanner. *OE* **55**: 096109 (2016)

[104] Lang V, Roch T, Lasagni A. World record in high speed laser surface microstructuring of polymer and steel using direct laser interference patterning. In *Proceedings Volume 9736, Laser-based Micro- and Nanoprocessing X*, San Francisco, California, USA, SPIE, 2016: 97360Z.

[105] Xing Y Q, Deng J X, Wu Z, Wu F F. High friction and low wear properties of laser-textured ceramic surface under dry friction. *Opt Laser Technol* **93**: 24–32 (2017)

[106] Eichstädt J, Römer G R B E, Veld A J H I. Towards Friction Control using laser-induced periodic Surface Structures. *Phys Procedia* **12**: 7–15 (2011)

[107] Rung S, Bokan K, Kleinwort F, Schwarz S, Simon P, Klein-Wiele J H, Esen C, Hellmann R. Possibilities of dry and lubricated friction modification enabled by different ultrashort laser-based surface structuring methods. *Lubricants* **7**(5): 43 (2019)

[108] van der Poel S, Mezera M, Römer G W, de Vries E, Matthews D. Fabricating laser-induced periodic surface structures on medical grade cobalt–chrome–molybdenum: Tribological, wetting and leaching properties. *Lubricants* **7**(8): 70 (2019)

[109] Alves-Lopes I, Almeida A, Oliveira V, Vilar R. Influence of laser surface nanotexturing on the friction behaviour of the silicon/sapphire system. *Opt Laser Technol* **121**: 105767 (2020)

[110] Wang Z, Zhao Q Z, Wang C W, Zhang Y. Modulation of dry tribological property of stainless steel by femtosecond laser surface texturing. *Appl Phys A* **119**(3): 1155–1163 (2015)

[111] Schille J. Experimental study on laser surface texturing for friction coefficient enhancement. *J Laser Micro* **10**(3): 245–253 (2015)

[112] Joshi G S, Putignano C, Gaudiuso C, Stark T, Kiedrowski T, Ancona A, Carbone G. Effects of the micro surface texturing in lubricated non-conformal point contacts. *Tribol Int* **127**: 296–301 (2018)

[113] Del Campo A, Greiner C, Arzt E. Contact shape controls adhesion of bioinspired fibrillar surfaces. *Langmuir* **23**(20): 10235–10243 (2007)

[114] Arzt E, Gorb S, Spolenak R. From micro to nano contacts in biological attachment devices. *PNAS* **100**(19): 10603–10606 (2003)

[115] Jin K J, Cremaldi J C, Erickson J S, Tian Y, Israelachvili J N, Pesika N S. Adhesives: biomimetic bidirectional switchable adhesive inspired by the gecko (adv. funct. mater. 5/2014). *Adv Funct Mater* **24**(5): 573 (2014)

[116] Huang W, Wang X. Biomimetic design of elastomer surface pattern for friction control under wet conditions. *Bioinspir Biomim* **8**(4): 046001 (2013)

[117] Drotlef D M, Stepien L, Kappl M, Barnes W J P, Butt H J, del Campo A. Insights into the adhesive mechanisms of tree frogs using artificial mimics. *Adv Funct Mater* **23**(9): 1137–1146 (2013)

[118] Kang M, Park Y M, Kim B H, Seo Y H. Micro- and nanoscale surface texturing effects on surface friction. *Appl Surf Sci* **345**: 344–348 (2015)

[119] Cañas N, Kamperman M, Völker B, Kroner E, McMeeking R M, Arzt E. Effect of nano- and micro-roughness on adhesion of bioinspired micropatterned surfaces. *Acta Biomater* **8**(1): 282–288 (2012)

[120] Sorrentino L, Marfia S, Parodo G, Sacco E. Laser treatment surface: An innovative method to increase the adhesive bonding of ENF joints in CFRP. *Compos Struct* **233**: 111638 (2020)

[121] Hamilton A, Xu Y, Kartal M E, Gadegaard N, Mulvihill D M. Enhancing strength and toughness of adhesive joints via micro-structured mechanical interlocking. *Int J Adhesion Adhesives* **105**: 102775 (2021)

[122] Wang W Q, Wang S Y, Zhang X G, Xu Y X, Tian Y T, Huang H. Enhanced aluminum alloy-polymer friction stir welding joints by introducing micro-textures. *Mater Lett* **295**: 129872 (2021)

[123] Costa H L, Oliveira M M Jr, de Mello J D B. Effect of debris size on the reciprocating sliding wear of aluminium. *Wear* **376–377**: 1399–1410 (2017)

[124] Liu Y F, Su J H, Tan C W, Feng Z W, Zhang H, Wu L J, Chen B, Song X G. Effect of laser texturing on mechanical strength and microstructural properties of hot-pressing joining of carbon fiber reinforced plastic to Ti_6Al_4V. *J Manuf Process* **65**: 30–41 (2021)

[125] Zhang K D, Guo X H, Wang C Y, Liu F, Sun L N. Effect of plasma-assisted laser pretreatment of hard coatings surface on the physical and chemical bonding between PVD soft and hard coatings and its resulting properties. *Appl Surf Sci* **509**: 145342 (2020)

[126] Liu X L, Song J F, Chen H C, Zhao G, Qiu J H, Ding Q J. Enhanced transfer efficiency of ultrasonic motors with polyimide based frictional materials and surface texture. *Sens Actuat A Phys* **295**: 671–677 (2019)

[127] Dufils J, Faverjon F, Héau C, Donnet C, Benayoun S, Valette S. Combination of laser surface texturing and DLC coating on PEEK for enhanced tribological properties. *Surf Coat Technol* **329**: 29–41 (2017)

[128] Liu X L, Qiu J H, Zhao G. Improved energy conversion efficiency of the ultrasonic motor with surface texture. *Ind Lubr Tribol* **70**(9): 1729–1736 (2018)

[129] Ito S, Takahashi K, Sasaki S. Generation mechanism of friction anisotropy by surface texturing under boundary lubrication. *Tribol Int* **149**: 105598 (2020)

[130] Wang N, Li D H, Song W L, Xiu S C, Meng X Z. Effect of surface texture and working gap on the braking performance of the magnetorheological fluid brake. *Smart Mater Struct* **25**(10): 105026 (2016)

[131] Santos L V, Trava-Airoldi V J, Corat E J, Nogueira J, Leite N F. DLC cold welding prevention films on a Ti_6Al_4V alloy for space applications. *Surf Coat Technol* **200**(8): 2587–2593 (2006)

[132] Tiner C, Bapat S, Nath S D, Atre S V, Malshe A. Exploring convergence of snake-skin-inspired texture designs and additive manufacturing for mechanical traction. *Procedia Manuf* **34**: 640–646 (2019)

[133] Sánchez J C, Estupiñán H, Toro A. Friction response of bioinspired AISI 52100 steel surfaces texturized by photochemical machining. *Surf Topogr*: *Metrol Prop* **9**(1): 014001 (2021)

[134] Xu Y, Li Z P, Zhang G Q, Wang G, Zeng Z X, Wang C T, Wang C C, Zhao S C, Zhang Y D, Ren T H. Electrochemical corrosion and anisotropic tribological properties of bioinspired hierarchical morphologies on Ti-6Al-4V fabricated by laser texturing. *Tribol Int* **134**: 352–364 (2019)

[135] Xu Y, Liu W, Zhang G Q, Li Z P, Hu H X, Wang C C, Zeng X Q, Zhao S C, Zhang Y D, Ren T H. Friction stability and cellular behaviors on laser textured Ti-6Al-4V alloy implants with bioinspired micro-overlapping structures. *J Mech Behav Biomed Mater* **109**: 103823 (2020)

[136] Gerthoffert J, Cerezo V, Thiery M, Bouteldja M, Do M T. A Brush-based approach for modelling runway friction assessment device. *Int J Pavement Eng* **21**(13): 1694–1702 (2020)

[137] Sabey B E, Williams T, Lupton G. Factors affecting the friction of tires on wet roads. *SAE Transactions* 1203-18 (1970)

[138] Mao C, Lv X, Yang X, Yang Z, Ma Y, Lv S. Design of convex-hull bionic tire tread compounds and mechanism on collaborative improvement of wet resistance and wear resistance. *J Appl Polym Sci* **138**(20): 50446 (2021)

[139] Jin X C, Hou C, Fan X L, Sun Y L, Lv J N, Lu C S. Investigation on the static and dynamic behaviors of non-pneumatic tires with honeycomb spokes. *Compos Struct* **187**: 27–35 (2018)

[140] Zhou H C, Zhai H H, Ding Y M, Wang G L. Numerical investigation of passive control flow to improve tire hydroplaning performance using a V-riblet non-smooth surface. *Adv Mech Eng* **9**(11): 168781401772724 (2017)

[141] Zhang Z W, Luan B, Liu X, Zhang M Q. Effects of surface texture on tire-pavement noise and skid resistance in long freeway tunnels: From field investigation to technical practice. *Appl Acoust* **160**: 107120 (2020)

[142] Zhu X Y, Yang Y, Zhao H D, Jelagin D, Chen F, Gilabert F A, Guarin A. Effects of surface texture deterioration and wet surface conditions on asphalt runway skid resistance. *Tribol Int* **153**: 106589 (2021)

[143] Moreno-Ríos M, Gallardo-Hernández E A, Yáñez-Escoto M J, Márquez-Tamayo L A, Iturbe-Salas E. Evaluation of surface modification in a steel track for the rubber tyred Metro. *Wear* **426–427**: 1265–1271 (2019)

[144] Kawazoe M, Miki N. Tactile samples with variable surface

textures to investigate tactile perception characteristic. *J Micromech Microeng* **30**(10): 105011 (2020)

[145] Renganathan P, Schwartz C J. Investigation of human perception of tactile graphics and its dependence on fundamental friction mechanisms. *Wear* **476**: 203729 (2021)

[146] Dione M, Watkins R H, Vezzoli E, Lemaire-Semail B, Wessberg J. Human low-threshold mechanoafferent responses to pure changes in friction controlled using an ultrasonic haptic device. *Sci Rep* **11**: 11227 (2021)

[147] Culbertson H, Kuchenbecker K J. Ungrounded haptic augmented reality system for displaying roughness and friction. *IEEE/ASME Trans Mechatron* **22**(4): 1839–1849 (2017)

[148] Etsion I. Modeling of surface texturing in hydrodynamic lubrication. *Friction* **1**(3): 195–209 (2013)

[149] Grützmacher P G, Profito F J, Rosenkranz A. Multi-scale surface texturing in tribology—Current knowledge and future perspectives. *Lubricants* **7**(11): 95 (2019)

[150] Spikes H A. Sixty years of EHL. *Lubr Sci* **18**(4): 265–291 (2006)

[151] Bi Z M, Mueller D W, Zhang C W J. State of the art of friction modelling at interfaces subjected to elastohydrodynamic lubrication (EHL). *Friction* **9**(2): 207–227 (2021)

[152] Marian M, Weikert T, Tremmel S. On friction reduction by surface modifications in the TEHL cam/tappet-contact-experimental and numerical studies. *Coatings* **9**(12): 843 (2019)

[153] Marian M, Grützmacher P, Rosenkranz A, Tremmel S, Mücklich F, Wartzack S. Designing surface textures for EHL point-contacts—Transient 3D simulations, meta-modeling and experimental validation. *Tribol Int* **137**: 152–163 (2019)

[154] Marian M, Weschta M, Tremmel S, Wartzack S. Simulation of microtextured surfaces in starved EHL contacts using commercial FE software. *Matls Perf Charact* **6**(2): MPC20160010 (2017)

[155] Gu C X, Meng X H, Xie Y B, Li P. A study on the tribological behavior of surface texturing on the nonflat piston ring under mixed lubrication. *Proc Inst Mech Eng Part J J Eng Tribol* **230**(4): 452–471 (2016)

[156] Profito F J, Tomanik E, Zachariadis D C. Effect of cylinder liner wear on the mixed lubrication regime of TLOCRs. *Tribol Int* **93**: 723–732 (2016)

Henara L. COSTA. She is a full professor at the Federal University of Rio Grande and a visiting professor at Federal University of Uberlândia and Federal University of Pelotas, Brazil. She obtained her B.S. (1992) and M.S. (1995) degrees in mechanical engineering from the Federal University of Uberlândia, Brazil, and her Ph.D. degree from Cambridge University, UK (2005). She has worked with tribology for over 25 years, with a main focus on reducing friction losses using surface modification and coatings or lubrication. She has authored over 180 manuscripts in journals, book chapters, and conference proceedings. She is a member of IFToMM and of editorial boards of a several tribology-related journals and the Brazilian representative at IEA/AMT. Currently she is the Editor-in-Chief of the journal "*Surface Topography: Metrology and Properties*".

Andreas ROSENKRANZ. He is a professor for materials-oriented tribology and new 2D materials in the Department of Chemical Engineering, Biotechnology and Materials at the University of Chile. His research focuses on the characterization, chemical functionalization, and application of new 2D materials. His main field of research is related to tribology (friction, wear, and energy efficiency), but in the last couple of years, he has also expanded his fields towards water purification, catalysis, and biological properties. He has published more than 100 peer-reviewed journal publications, is a fellow of the Alexander von Humboldt Foundation, and acts as a scientific editor for different well-reputed scientific journals including *Applied Nanoscience* and *Frontiers of Chemistry*.